SAE International

Development of a Simulation Model to Analyze the Effect of Thermal Management on Battery Life

2012-01-0671
Published
04/16/2012

Tugce Yuksel and Jeremy Michalek
Carnegie Mellon Univ.

doi:10.4271/2012-01-0671

ABSTRACT

Battery life and performance depend strongly on temperature; thus there exists a need for thermal conditioning in plug-in vehicle applications. The effectiveness of thermal management in extending battery life depends on the design of thermal management used as well as the specific battery chemistry, cell and pack design, vehicle system characteristics, and operating conditions. We examine the case of an air cooled plug-in hybrid electric vehicle battery pack with cylindrical $LiFePO_4$/graphite cell design and address the question: How much improvement in battery life can be obtained with passive air cooling? To answer this question, a model is constructed consisting of a thermal model that calculates temperature change in the battery and a degradation model that estimates capacity loss. A driving and storage profile is constructed and simulated in two cities - Miami and Phoenix - which have different seasonal temperatures. The results suggest that air cooling may extend battery life by 5% in Miami, characterized by higher average temperatures, and by 23% in Phoenix, characterized by higher peak temperatures. Thus, thermal management appears to have the greatest effect in regions with high peak temperatures, even if the region has lower average temperatures.

INTRODUCTION

Plug-in hybrid electric vehicles (PHEVs) have the potential to reduce operating cost, greenhouse gas (GHG) emissions, and petroleum consumption in the transportation sector. Despite these benefits, there are barriers to market penetration and high battery cost is among the most significant [1,2,3,4]. For many plug-in vehicles, the battery is the most expensive component, so if batteries need to be replaced before the vehicle's end of life, cost competitiveness suffers. Although different design choices can lead to different battery EOL criteria [5], EOL is typically defined as the time when 20% capacity loss or 30% internal resistance growth is reached, whichever comes first. According to the goals set by US Advanced Battery Consortium (USABC), a PHEV battery is targeted to have 15 years of calendar life and 300,000 cycles of cycle life [6].

Battery life depends on the inherent characteristics of the battery such as its technology and design. Currently, PHEVs use Li-ion chemistries due to superior power and energy characteristics. However, battery characteristics such as power, energy, life and safety can vary among different type of Li-ion batteries, depending on the cell design and the material chemistries used in cathode and anode. Although there are various materials being used as cathode material, the most commonly used anode material is graphite. Therefore, in the literature, Li-ion chemistry is often specified by its cathode material.

Apart from the specific type and design of the battery, the conditions and stress factors during storage and cycling also affects how quickly the battery will degrade. There are various factors that affect battery life such as time, charge/ discharge rate, temperature, and state of charge (SOC). How these factors affect degradation depends on battery chemistry. Therefore modeling degradation is a complex and challenging task. There is no single life model that models degradation of all Li-ion chemistries.

One of the stress factors that is known to affect degradation rate in all Li-ion chemistries is temperature. Usually, the relationship between degradation and temperature can be formulated by an Arrhenius type behavior where degradation rate increases exponentially with temperature [7,8,9]. However, the exact relation depends on the specific

electrochemistry, design, and conditioning of the battery. Degradation models used in the literature are usually not derived from physical fundamentals but obtained from experimental data. These data are obtained mostly by performing experiments on cells rather than battery packs, and studies cover a wide variety depending on the cell electrochemistry, capacity and power characteristics. Two chemistries that have been extensively tested in the public literature are $LiNi_xCo_yAl_{(1-x-y)}O_2$ (NCA) and $LiFePO_4$ (LFP) chemistries.

Hall et al. [10] tested NCA cells used in satellite applications and found that the main degradation mechanism is the lithium loss due to the formation of a layer between cathode and electrolyte called solid electrolyte interface (SEI). In the same study, it was also shown that during storage impedance growth has a $t^{1/2}$ dependence, where t represents time, and during cycling a component linear with time is added to this behavior. The same type of storage behavior of impedance growth in this chemistry was also reported by Thomas et al. [8] in which the temperature dependence of impedance growth rate was modeled using an Arrhenius type of equation. The Gen 2 Performance Evaluation Final Report [11] by Advanced Technology Development Program showed that the capacity loss in this chemistry depends not only on temperature but also on SOC exponentially.

$LiFePO_4$ chemistry is promising due to its safety and longer life characteristics [12,13,14]. Liu et al. [15] showed that, similar to NCA chemistry, the main mechanism of degradation in $LiFePO_4$ batteries is active lithium loss during the formation of the SEI layer. They also showed that, there is not an appreciable impedance growth in this chemistry. Peterson et al. [16] tested $LiFePO_4$ chemistry cells manufactured by A123 Systems at a single ambient temperature and reported that degradation is not dependent upon the depth of discharge (DOD). Wang et al. [9] performed similar tests at various temperatures and showed that capacity loss can be related to temperature and *ampere-hour (Ah)* processed. They modeled the temperature dependence with an Arrhenius type of equation and dependence on Ah-processed by an $Ah^{0.552}$ behavior. Li et al. [17] tested and evaluated the degradation in cells by considering the effects of coupling between stress factors. They analyzed the effects of temperature, charge/discharge rate, end of charge voltage and end of discharge voltage, and showed that there is a coupling effect between each of these factors. Coupling is related to stress levels and there exists a critical stress level at which coupling can be neglected. Finally, A123 Systems provided capacity loss with cycling and storage at different temperatures for their $LiFePO_4$ chemistry ANR26650M1 cells [18, 19].

The exponential effect of temperature on degradation in both chemistries shows the necessity to control the battery temperature in PHEVs. Thermal management techniques can be classified depending on the purpose (heating only versus heating and cooling), the source (passive if ambient air is used without any pre-heating/cooling before entering the battery, active if a heating/cooling device is built-in to the system) and the cooling medium (air versus liquid)[1] [20]. To evaluate the performance of a thermal management system, thermal models of the battery and thermal management can be used. Ma et al. [21] calculated the temperature increase and temperature distribution in a PHEV battery pack using a finite element thermal model. Kim and Paseran [22] compared air and liquid cooling thermal management techniques. They concluded that liquid cooling provides much better heat transfer rate, however liquid cooling increases complexity and cost, as well as maintenance requirements.

Most of the studies on this topic restrict scope to either battery degradation or battery thermal management. Studies of the effect of thermal management on battery life are rare. Gross and Clark [23] aimed to analyze the effect of thermal management on battery life in a battery electric vehicle (BEV). They compared two cases: (1) cell heat is transferred to ambient environment; (2) active thermal management, where the coolant is forced to be at a temperature below ambient. They used a generic formulation for degradation which they assumed to be applicable to all battery chemistries. Experiment driven estimations for heat transfer rates for each case were used to calculate the change in battery temperature. They found that active cooling improves battery life by 4.4% to 6.5%, where values vary depending on the region.

We construct an integrated thermal management and battery degradation model for an air cooled PHEV battery pack with $LiFePO_4$/graphite cell chemistry to address the question: "How much improvement can be obtained in battery life with simple air cooling?". A daily driving and storage scenario is posed and applied under different weather conditions in two cities, Miami and Phoenix, and battery life is calculated for two cases: air cooling versus no cooling. Preliminary results, limitations, and future work are discussed.

---

[1] Note that, in this study, the air cooling systems currently being used in hybrid electric vehicles are referred as 'passive', even though the ambient air is cooled or heated by vehicle's air conditioning and heating system before going into the battery. In this study, the 'active' and 'passive' system definitions proposed by Paseran [20] are used. According to his definition, a thermal management system is called 'passive' unless there is an active component (evaporators, heating cores, engine coolant) in the thermal management system itself. Therefore, using air conditioning system to pre-cool the air does not make the thermal management system itself 'active'.

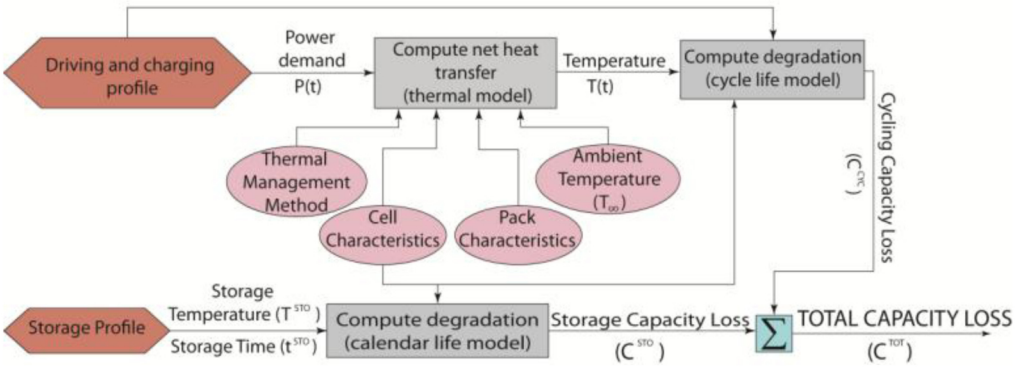

Figure 1. Schematic view of simulations to calculate battery life.

ANALYSIS

DESCRIPTION OF THE SIMULATIONS

Simulation Procedure

Using the thermal and life models, daily simulations for a vehicle use and storage profiles are performed. These simulations are summarized in Figure 1. Battery life is calculated by computing capacity loss in two parts: cycling capacity loss, which corresponds to the loss during driving and charging, and storage capacity loss.

To calculate cycling degradation, driving and charging power demand at each time step are given as inputs to the thermal model. Thermal model calculates the rate of change of battery temperature by computing heat generated inside and heat transferred from the battery for two separate cases: (1) the battery is being cooled by an air cooling thermal management system, and (2) there is no thermal management system to cool the battery. In these calculations, the initial battery temperature is assumed to be equal to ambient temperature. The net heat transfer is used to calculate the change in battery temperature. Temperature is an input to the cycle life model, which computes capacity loss at each time step using temperature, time and current drawn from the battery as inputs. Battery current is obtained based on the driving and charging profile. The cycling life model also takes the previous capacity loss history into account during calculations. The set of calculations performed at each time step are given in Equations 1 and 2.

$$T_t = T_{t-1} + \dot{T}_{t-1}\left(\dot{Q}^{\mathrm{TR}}_{t-1}, \dot{Q}^{\mathrm{GEN}}_{t-1}\right) \cdot \Delta t$$

$$\begin{cases} \dot{Q}^{\mathrm{TR}}_{t-1} = \dot{Q}^{\mathrm{TR}}_{t-1}(T_\infty, V_{\mathrm{air}}, \rho_{\mathrm{air}}, c_{\mathrm{air}}, A_{\mathrm{cell}}) \\ \dot{Q}^{\mathrm{GEN}}_{t-1} = \dot{Q}^{\mathrm{GEN}}_{t-1}(I_{t-1}, R_{t-1}) \end{cases} \quad (1)$$

$$C^{\mathrm{CYC}}_t = C^{\mathrm{CYC}}_{t-1} + \Delta C^{\mathrm{CYC}}_{t-1}\left(C^{\mathrm{CYC}}_{t-1}, I_{t-1}, T_{t-1}, \Delta t\right) \quad (2)$$

In these equations, subscript t refers to time step t. T is the battery temperature, $\dot{T}$ is the change in battery temperature which is assumed to be constant over Δt, Q^{GEN} is rate of the heat generated in the battery, Q^{TR} is the rate of heat removed from the battery, T_∞ is the cabin air temperature entering into pack, V_{air}, ρ_{air} and c_{air} are air speed, density and constant specific heat respectively, A_{cell} is the heat transfer area of a cell, C^{CYC} is percent cycling capacity loss, I is the current drawn from the battery, and R is internal resistance.

Daily storage fade (capacity loss when the battery is at rest) is evaluated using the calendar life model, assuming that the battery is at ambient temperature when it is at rest. The total capacity fade at the end of the day is the sum of cycling and capacity fade. Simulations corresponding to duration of one week are performed at each seasonal ambient temperature. It was observed from one week simulations that capacity fade is not constant on daily basis, but there is a power function relationship between the number of days and capacity loss, where the power is equal to ½. Using this fact, capacity fade profile during the simulated one week period is extrapolated to estimate fade during the remainder of the season. Battery life is defined as the number of years passed until a total capacity loss of 20% reached. The evaluated system and the calculations performed at each block of the simulation are detailed in the following sections.

Daily Usage Profile

The simulated vehicle - which is considered to have the specifications of a PHEV conversion of a 2004 Toyota Prius - is assumed to make two trips in a day with the Urban Dynamometer Driving Schedule (UDDS). The dynamic power profile needed to achieve this driving cycle is derived by calculating the acceleration force as well as the resistance forces such as air and rolling resistances as described in Peterson, 2010 [16]. After both trips are completed, the battery is charged at a constant current of 4.6 amperes up to 90% SOC, after which there is a rest period until the next trip. This daily profile is given in Table 1 and simulated for two cities: Miami and Phoenix. These two cities were selected to

satisfy modeling constraints while comparing cities with different levels of seasonal variation. The ambient temperature profile is obtained by dividing a year into four seasons and using the average temperatures of each season as daily ambient temperature. The seasonal average temperatures are given in Table 2.

Table 1. Daily Usage Profile Simulated.

	Duration
Trip with 2xUDDS	46 min
Constant current charge (4.6 A)	~3.43 hours
Rest at ambient temperature	~19.8 hours

Table 2. Seasonal Average Temperatures in Simulated Cities [°C] [24].

	Winter	Spring	Summer	Fall
Miami	22	26	27.5	25
Phoenix	15	26	33	17

THERMAL MANAGEMENT MODELING

Battery Pack

In this study, a battery pack similar to the A123 Systems Hymotion Li-ion battery pack is modeled. This is a kit to convert a hybrid electric vehicle (HEV) to a PHEV, used in the Toyota Prius conversion. This pack consists of 14 modules, each module having 44 cylindrical cells, as shown in Figure 2 [25]. The pack is cooled by a fan which draws cabin air to the battery as shown in Figure 3 [20, 26]. Air is divided into parallel flows so that each module has the same amount of air passing through [21]. Therefore, in this study, only one module is modeled to represent the whole battery pack. The fan in Prius HEV works with an on-off control strategy and is not turned on until the battery temperature reaches 35°C. Then it turns off again if the battery temperature falls to 33°C [26]. In this study, the Hymotion pack fan is assumed to have the same on-off control strategy with Prius HEV. During driving and charging, it is assumed that the driver conditions the cabin and keeps the cabin temperature at 24°C all the time. Therefore, during driving and charging, the air inlet temperature is 24°C. When the battery is at rest, cabin air temperature is presumed to be equal to the ambient temperature. It is assumed that air enters the pack at a constant flow rate when the fan is on.

Figure 2. A123 Hymotion Li-ion conversion battery pack.

Table 3. Hymotion Battery Pack Specifications [25].

	Pack	Single Module
Energy	25.3 Ah	25.3 Ah
Capacity	~5 kWh	~357 Wh
Charging time	5.5 hours	5.5 hours
Maximum charging current	10 A	10 A

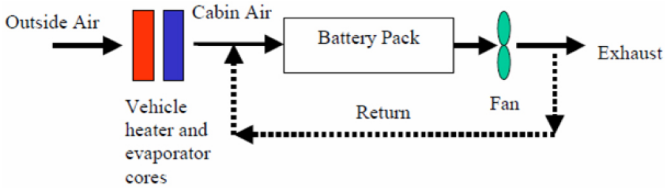

Figure 3. Air cooling thermal management system [20].

Heat Generated in the Battery

The heat generated inside the pack is modeled as:

$$\dot{Q}^{\mathrm{GEN}} = NI^2R \qquad (3)$$

I is the current drawn from each cell, which is calculated from the power load on the battery using the relation $I=P/V$. R is the internal resistance of the cell, a function of temperature T and state-of-charge (SOC). Internal resistance maps are derived from the voltage-versus-capacity graphs given in the manufacturer's specifications [18]. N is the number of cells in the battery.

Heat Transferred from the Battery

Although the real cell arrangement in the pack is neither entirely aligned nor staggered, it has a mostly staggered arrangement; therefore the pack is modeled as a staggered bank of tubes as given in Figure 4. It is assumed that the cells are constant temperature surfaces and also the temperature distribution is uniform throughout the module, since providing uniform temperature distribution is a design criterion in battery thermal management systems [20,27].

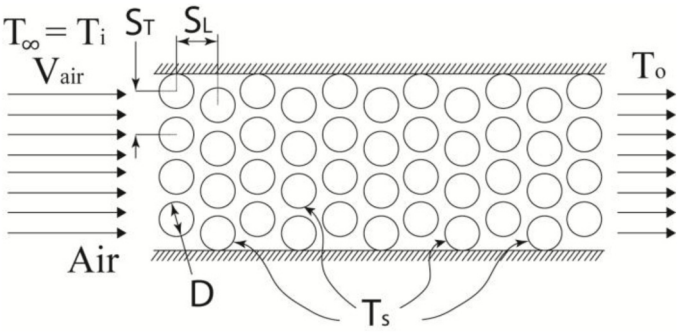

Figure 4. Staggered cell arrangement inside a module.

When fan is turned on, there is a forced air flow over the cells. To find the heat removed by this forced flow, the overall heat transfer coefficient *h* can be calculated by:

$$h = N_{\mathrm{Nu}} k/D \tag{4}$$

where N_{Nu} is the Nusselt number, k is thermal conductivity of air and D is the cell diameter. For the assumed staggered configuration, the Nusselt number can be estimated using Zukauskas correlation [28, 29]:

$$N_{\mathrm{Nu}} = C N_{\mathrm{Re,max}}^{m} N_{\mathrm{Pr}}^{0.36} \left(N_{\mathrm{Pr}}/N_{\mathrm{Pr,s}}\right)^{1/4} \tag{5}$$

$N_{\mathrm{Re,max}}$ is the Reynolds number calculated at maximum air velocity, C and m are constants obtained empirically and tabulated for $N_{\mathrm{Re,max}}$ and N, N_{pr} is the Prandtl number. $N_{\mathrm{Re,max}}$ and N_{pr} are calculated at the film temperature, T_f, which is defined as:

$$T_f \equiv (T_{\mathrm{s}} + T_{\mathrm{i}})/2 \tag{6}$$

where T_{s} is the cell surface temperature and T_{i} is inlet air temperature (which is equal to the cabin air temperature). $N_{\mathrm{pr,s}}$ is calculated at T_{s}. Once h is calculated, the rate of heat transfer from the battery can be computed as:

$$\dot{Q}^{\mathrm{TR}} = N h \pi D \Delta T_{lm} L \tag{7}$$

L is the length of a cell and ΔT_{lm} is the log mean temperature difference defined as:

$$\Delta T_{lm} = \frac{(T_s - T_i) - (T_s - T_o)}{ln\left(\frac{T_s - T_i}{T_s - T_o}\right)} \tag{8}$$

T_o is the temperature of air leaving the battery, and can be calculated by using the relation given in Equation 9, which can be obtained by equating the heat transferred from the cell surfaces to air (Equation 7) to the heat carried away by air ($m_{air} c_{air} \Delta T_{air}$):

$$\left(\frac{T_s - T_o}{T_s - T_i}\right) = exp\left(-\frac{\pi D N h}{\rho_{air} V_{air} N_T S_T c_{air}}\right) \tag{9}$$

where, N_T is the number of cells in transverse direction, S_T is the transverse pitch shown in Figure 4, V_{air} is the air speed, ρ_{air} is air density and is air constant specific heat.

When the fan is turned off or when there is no thermal management system at all, during driving and charging, the amount of heat removed by natural convection is neglected. When the vehicle is at rest, it is assumed that battery temperature comes to equilibrium with ambient temperature immediately. This assumption is reasonable if fan is left on after the vehicle stops until the battery temperature drops to ambient. However, for no thermal management case, storage fade is underestimated with this assumption, so we underestimate the benefit of thermal management over no thermal management.

Calculation of the Battery Temperature

Once heat generation and heat transfer rates are found, $\dot{T}$ can be computed at each time step as:

$$\dot{T} = (\dot{Q}^{\mathrm{GEN}} - \dot{Q}^{\mathrm{TR}})/(m \cdot c_p) \tag{10}$$

where m is the module mass and c_p is the module thermal capacity. The battery temperature at the end of each time step can be calculated using Equation 1.

BATTERY LIFE MODELING

Capacity loss and internal resistance growth are two measures of battery life and affected by factors like SOC[2], C-rate[3], and temperature. Although various studies evaluate battery degradation, no studies were found that characterizes the effects of all factors that influence degradation. Besides, degradation behavior depends on battery chemistry; therefore any life model developed should be chemistry specific.

We focus on $LiFePO_4$ chemistry because it is used in the Hymotion battery pack, it is studied extensively in public literature [9, 15, 16, 17], and negligible impedance growth [15, 16] offers simplified life modeling focused on capacity

[2] State of Charge (SOC) is the amount of capacity remained in the battery after discharge, expressed as a percentage of the total capacity

[3] C-rate expresses the rated capacity value of a battery. For example 1C discharge rate means that the battery will deliver its nominal capacity in 1 hour.

loss criteria. Cycling and storage capacity loss mechanisms are assumed to be decoupled and modeled separately.

Cycling Fade

Cycling capacity fade is modeled using data from A123 Systems specification sheets for their $LiFePO_4$/graphite based ANR26650M1 cells [18], in which they provide constant charge/discharge capacity loss versus number of cycles at three different temperatures: 25, 45 and 60°C. The constant discharge/charge duty cycle is quite different than the UDDS cycle simulated in this study. Therefore, using number of cycles in the cycling degradation model would need misleading results. In this paper, to reduce the discrepancy due to different duty cycles, the number of cycles is converted to Ah- processed (I^{PR}), the integral of absolute value of current over time. The literature suggests that capacity loss is a function of $(I^{PR})^z$ where z is a value near 0.5 [9]. Using an Arrhenius type of relation for temperature dependence, the fit given in Equation 11 is obtained, where R_{gas} is the universal gas constant, and T is the battery temperature in Kelvin.

$$C^{CYC} = A \cdot \exp\left(-B/\left(R_{gas} \cdot T\right)\right)(I^{PR})^{0.55} \quad (11)$$

Using least-squares fit to data points extracted from [18] gives:

$$A = 1.1443 \times 10^6 \quad \text{and} \quad B = 4.257 \times 10^4$$

This model fits the data with $R^2 = 0.98$. Figure 5 shows the data points and the fit.

Storage Fade

Using data from manufacturer's specifications [19], which gives the storage fade with time at four different temperatures, the fit in Equation 12 is obtained, again using least squares regression.

$$\begin{cases} C^{STO} = (0.23T - 67)log10(t) - (0.3T - 88.95), T \le 45°C \\ C^{STO} = (0.23T - 67)log10(t) - (0.013T + 2.36), T > 45°C \end{cases} \quad (12)$$

This model form is selected because it is observed from data that there is a linear relationship between the percent capacity loss and logarithm of time (in days). Data and fit at storage is given in Figure 6.

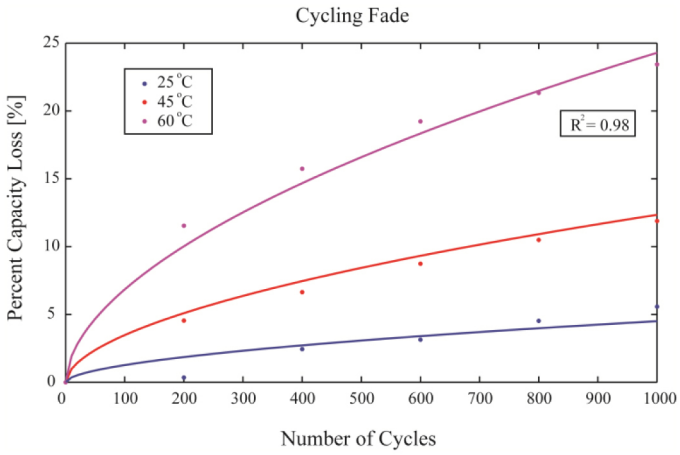

Figure 5. Capacity fade with cycling-Data and fit.

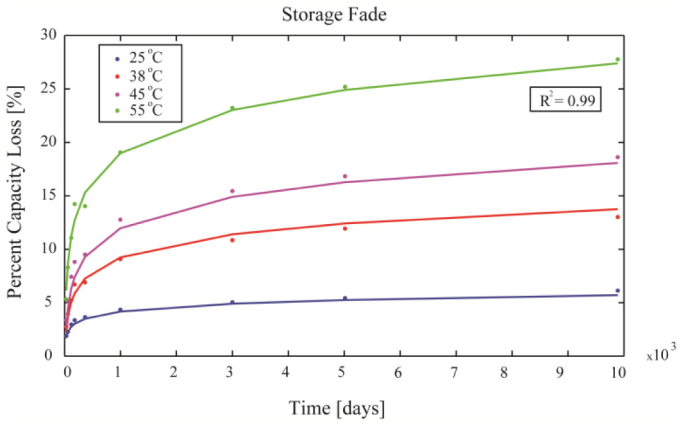

Figure 6. Capacity Fade at Storage-Data and Fit.

RESULTS AND DISCUSSION

Figures 7 and 8 give the daily temperature profile during usage (2 trips and charging) in Miami and Phoenix respectively. Fluctuations observed around 33°C are due to the thermal fan on-off control strategy. Temperature rise during charging is observed to be relatively low. When there is no thermal management system, the temperature reaches a maximum value of 39°C in Miami, whereas in Phoenix the maximum temperature is about 43°C in summer. Thermal management maintains the battery temperature below 35°C in both cities.

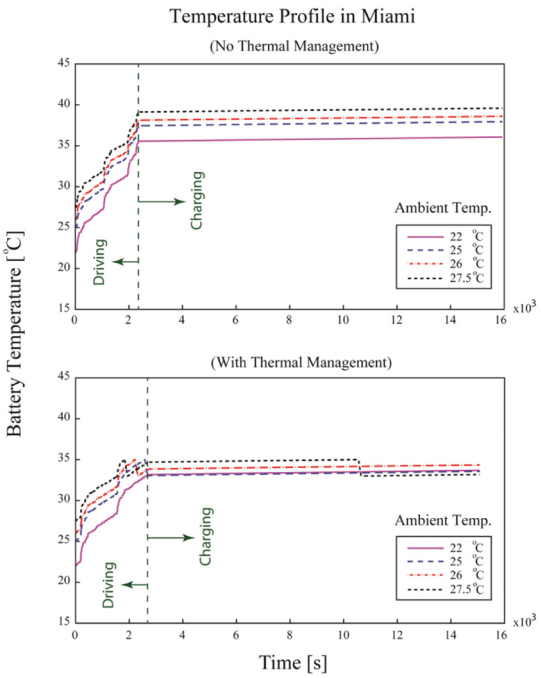

Figure 7. Temperature profile obtained from driving and charging simulations in Miami. (Battery temperature at rest is not shown in this graph since it is simply assumed to be equal to ambient temperature.)

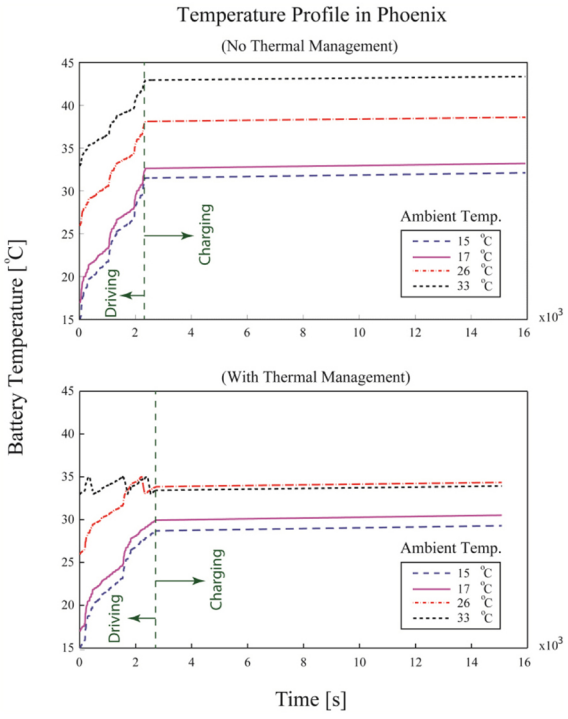

Figure 8. Temperature profile obtained from driving and charging simulations in Phoenix. (Battery temperature at rest is not shown in this graph since it is simply assumed to be equal to ambient temperature.)

The change in capacity loss over 30 years is calculated for both cases and the results are presented in Figures 9 and 10 for Miami and Phoenix respectively. The results designate that if a thermal management system is used, the battery has a longer life in Phoenix than in Miami. When thermal management is not used in Miami, battery life decreases only one year, whereas a decrease of 3 years is observed in Phoenix.

Average seasonal temperatures in Phoenix are lower than or equal to the corresponding temperatures in Miami except during the summer season. However, when there is no thermal management to cool the battery, battery life in Phoenix is ~3 years shorter than the battery life in Miami. This shows the importance of high peak temperatures on battery life, even if they are observed only in one fourth of the year. The effect of this high temperature season could be reduced by cooling the battery with air in Phoenix, where air cooling provides an estimated battery life improvement of 23%. However, in Miami the improvement in battery life is only 5%, corresponding to 1 year of additional battery life. This shows that the life improvement that can be obtained with a specific type of thermal management system, and/or the decision to upgrade a thermal management system depends on the region where the vehicle is being used. The results also indicate that battery thermal management is most critical for peak temperatures. The results are summarized in Table 4.

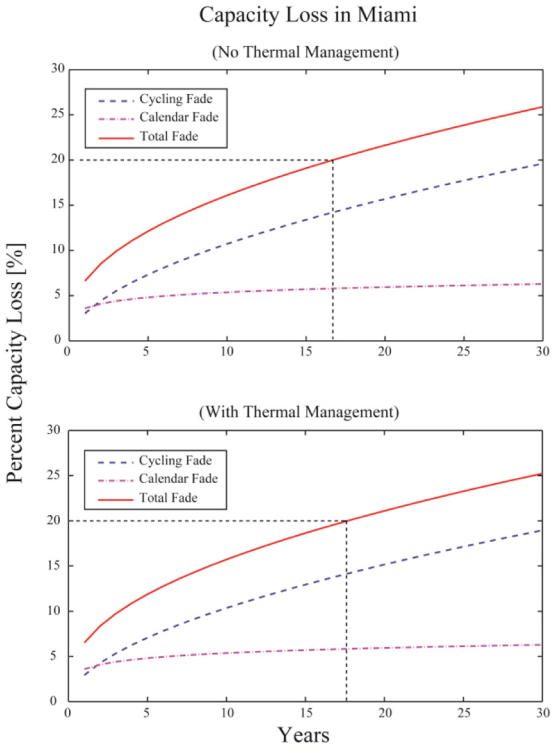

Figure 9. Capacity Loss in Miami.

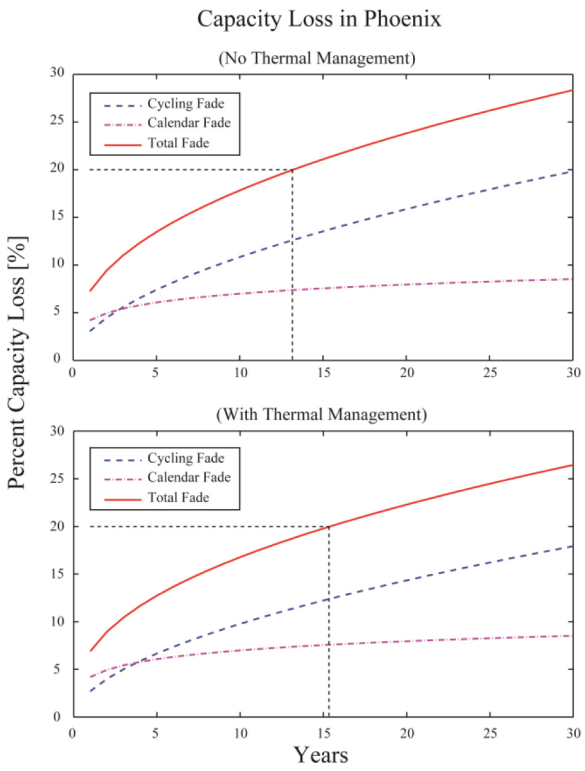

Figure 10. Capacity Loss in Phoenix.

Table 4. Summary of Results

	Max. Battery Temperature		Battery Life	
	Miami	Phoenix	Miami	Phoenix
No Thermal Management	39 °C	43 °C	17 years	13 years
With Thermal Management	35 °C	35 °C	18 years	16 years

ASSUMPTIONS/MODEL LIMITATIONS

This paper presents the preliminary results of an ongoing study evaluating the effect of thermal management on battery life. The models presented here therefore have some limitations that will be addressed in future work. In particular, the battery life models used in this study are derived using data for a limited range of temperatures, and trends are extrapolated for lower temperatures. When storage life models are extrapolated to temperatures lower than 15°C, counterintuitive trends are observed. We selected cities to avoid temperatures below 15°C; however, because degradation rates are primarily driven by peak temperatures, errors in degradation rates at low temperatures may be less critical. Secondly, real-world driving profiles, which tend to be more aggressive than EPA test cycles, should be simulated to obtain more realistic battery life results. In addition, since results significantly depend on peak temperatures, higher resolution temperature data, such as hourly or daily temperature averages should be used instead of seasonal averages to improve estimates.

In thermal management, providing uniform temperature distribution is a design criterion. In this study, it was assumed that the system modeled satisfies this criterion by maintaining a negligible temperature variance across the pack. However, since temperature variance will cause some cells degrade faster than others, it is still necessary to check the validity of this assumption in future studies by using tools like computational fluid dynamics analysis. In addition, natural convection and pack conduction, ignored in this study, may be important when there is no forced air flow over the cells. Moreover, the assumption that battery temperature reaches ambient immediately when the vehicle is at rest underestimates storage fade. If the fan runs using ambient air after parking, we estimate that the pack can be cooled to within 5% of ambient temperature in less than 25 minutes for an extreme case of 30°C battery temperature at the moment the vehicle stops and 15°C ambient temperature. This time is reduced if pre-conditioned cabin air is used or if the temperature difference is smaller. Because 25 minutes is less than 5% of total storage time, we expect the effect of this simplification on calendar fade to be second order. However, for the case of no thermal management, the time needed to cool down to ambient temperature would be longer, causing increased storage fade. By ignoring the time taken for the battery to cool down when at rest, we underestimate the benefit of thermal management over no thermal management. Therefore, it is necessary in future work to assess the actual temperature profile of the battery at rest and use that profile in storage fade calculations. We also explore only limited thermal control strategies, assuming fixed threshold temperatures for turning the thermal management system on and off. We observe that decreasing the fan onset temperature by 2°C can extend battery life by as much as 10 percent, so further examination of control parameters is necessary to understand optimal operating conditions for comparison. Likewise, changing air flow rate may affect results significantly. In future work, we intend to analyze sensitivity of results to these variables and address the model limitations described above.

SUMMARY/CONCLUSIONS

We present an analysis to estimate the improvement in battery life in PHEVs by air-cooling the battery using an integrated thermal management and battery degradation model for a battery pack with $LiFePO_4$/graphite cell chemistry. Daily simulations were performed in two cities, Miami and Phoenix, using a constructed daily driving and charging profile and seasonal average ambient temperatures. Thermal management provided a better improvement in

Phoenix, where higher peak temperatures are observed. It was also observed that the battery life in Phoenix is shorter than in Miami even though the temperature in Phoenix is lower than Miami half of the year. These results suggest that the improvement that can be obtained by thermal management depends on the region where the vehicle is being used, and battery thermal management is most critical for peak temperatures. Future work will address the identified model limitations to improve accuracy of estimates and comparisons.

REFERENCES

1. Michalek, J., Chester, M., Jaramillo, P., Samaras, C., Shiau, N. & Lave, L., "Valuation of Plug-in Vehicle Life Cycle Air Emissions and Oil Displacement Benefits," *Proceedings of the National Academy of Sciences*, **108**(40): 16554-16558, 2011, doi: 10.1073/pnas.1104473108.

2. Axsen, J., Burke, A.F., & Kurani, K.S., "Batteries for PHEVs: Comparing Goals and State of Technology," *Electric and Hybrid Vehicles: Power Sources, Model, Sustainability, Infrastructure and the Market*, ed Pistoia, G. (Elsevier, Amsterdam, The Netherlands), 2010, pp 405-427.

3. Delucchi, M. & Lipman, T., "Lifetime cost of battery, fuel-cell, and plug-in hybrid electric vehicles," *Electric and Hybrid Vehicles: Power Sources, Model, Sustainability, Infrastructure and the Market*, ed Pistoia, G (Elsevier, Amsterdam, The Netherlands), 2010, pp 19-60.

4. Markel, T., Brooker, A., Gonder, J., O'Keefe, M., Simpson, A. & Thornton, M., "Plug-in Hybrid Vehicle Analysis," *National Renewable Energy Laboratory, Milestone Report*, 2006.

5. Shiau, N., Kaushal, N., Hendrickson, C., Peterson, S., Whitacre, J., & Michalek, J., "Optimal Plug-In Hybrid Electric Vehicle Design and Allocation for Minimum Life Cycle Cost, Petroleum Consumption, and Greenhouse Gas Emissions," *Journal of Mechanical Design*, **132**:091013-1, 2011, doi: 10.1115/1.4002194.

6. Peseran, A.A., Markel, T., Tataria & Howell, D., "Battery Requirements for Plug-In Hybrid Electric Vehicles-Analysis and Rationale," presented at 23rd International Electric Vehicle Symposium, Anaheim, California, USA, December 2-5, 2007.

7. Broussely, M., "Aging Mechanisms and Calendar-Life Predictions in Lithium-Ion Batteries," *Advances in Lithium-Ion Batteries*, ed van Schalkwijk, W.A & Scrosati, B (Kluwer Academic/Plenum Publishers, New York), 2002, pp 393-432.

8. Thomas, E.V., Bloom, I., Christophersen, J.P. & Battaglia, V.S., "Statistical methodology for predicting the life of lithium-ion cells via accelerated degradation testing," Journal of Power Sources, **184**: 312-317,2008, doi: 10.1016/j.jpowsour.2008.06.017.

9. Wang, J., Liu, P., Hicks-Garner, J., Sherman, E., Soukiazian, S., Verbrugge, M., Tataria, H., Musser, J. & Finamore, P., "Cycle-life model for graphite-LiFePO4 cells," Journal of Power Sources, **196**: 3942-3948, 2011, doi: 10.1016/j.jpowsour.2010.11.134.

10. Hall, J.C., Lin, T., Brown, G., Biensan, P. & Bonhomme, F., "Decay Process and Life Predictions for Lithium Ion Satellite Cells," presented at 4th International Energy Conversion Engineering Conference and Exhibit, California, USA, June 26-29, 2006.

11. Christophersen, J.P., Bloom, I., Thomas, E.V., Gering, K.L., Henriksen, G.L., Battaglia, V.S., & Howell, D., "Advanced Technology Development Program For Lithium-Ion Batteries: Gen 2 Performance Evaluation Final Report," Idaho National Laboratory, July 2006.

12. Broussely, M., "Battery Requirements for HEVs, PHEVs, and EVs: An Overview," *Electric and Hybrid Vehicles: Power Sources, Model, Sustainability, Infrastructure and the Market*, ed Pistoia, G (Elsevier, Amsterdam, The Netherlands), 2010, pp 305-347.

13. Zhang, Y., Wang, C., & Tang, X., "Cycling degradation of an automotive $LiFePO_4$ lithium-ion battery," *Journal of Power Sources*, **196**: 1513-1520, 2011, doi: 10.1016/j.jpowsour.2010.08.070.

14. Amine, K., Liu, J., & Belharouak, I., "High-temperature storage and cycling of C- $LiFePO_4$/graphite Li-ion cells," *Electrochemistry Communications*, **7**: 669-673, 2005, doi: 10.1016/j.elecom.2005.04.018.

15. Liu, P., Wang, J., Hicks-Garner, J., Sherman, E., Soukiazian, S., Verbrugge, M., Tataria, H., Musser, J. & Finamore, P., "Aging Mechanisms of $LiFePO_4$ Batteries Deduced by Electrochemical and Structural Analyses," *Journal of The Electrochemical Society*, **157**(4): A499-A507, 2010, doi: 10.1149/1.3294790.

16. Peterson, S., Apt, J. & Whitacre, J.F., "Lithium-ion battery cell degradation resulting from realistic vehicle and vehicle-to-grid utilization," *Journal of Power Sources*, **195**: 2385-2392, 2010, doi: 10.1016/j.jpowsour.2009.10.010.

17. Li, Z., Lu, L., Ouyang, M. & Xiao, Y., "Modeling the capacity degradation of LiFePO4/graphite batteries based on stress coupling analysis," *Journal of Power Sources*, **196**: 9757-9766, 2011, doi: 10.1016/j.jpowsour.2011.07.080.

18. A123 Systems, "ANR26650M1A Cells Data Sheet" http://www.a123systems.com/products-cells-26650-cylindrical-cell.htm.

19. A123 Systems, "Development of Battery Packs for Space Applications," presented at NASA Aerospace Battery Workshop, USA, November 27-29, 2007.

20. Pesaran, A.A., "Battery Thermal Management in EVs and HEVs: Issues and Solutions," presented at Advanced Automotive Battery Conference, Nevada, USA, February 6-8, 2001

21. Ma, Y., Teng, H., and Thelliez, M., "Electro-Thermal Modeling of a Lithium-ion Battery System," *SAE Int. J. Engines* 3(2):306-317, 2010, doi:10.4271/2010-01-2204.

22. Kim, G.H. & Peseran, A.A., "Battery Thermal Management System Design Modeling," presented at 22nd International Battery, Hybrid and Fuel Cell Electric Vehicle Conference and Exhibition, Yokohoma, Japan, October 23-28, 2006.

23. Gross, O. and Clark, S., "Optimizing Electric Vehicle Battery Life through Battery Thermal Management," *SAE Int. J. Engines* 4(1):1928-1943, 2011, doi:10.4271/2011-01-1370.

24. NOAA Satellite and Information Service, "U.S. Climate Normals", http://cdo.ncdc.noaa.gov/cgi-bin/climatenormals/climatenormals.pl.

25. A123 Systems, "Hymotion L5 Plug-in Conversion Module Spec-sheet", http://www.hymotion.com/hymotion/pdf/L5_SpecSheet.pdf.

26. Zolot, M., Pesaran, A., and Mihalic, M., "Thermal Evaluation of Toyota Prius Battery Pack," SAE Technical Paper 2002-01-1962, 2002, doi:10.4271/2002-01-1962.

27. Pesaran, A.A., Burch, S., & Keyser, M., "*An Approach for Designing Thermal Management Systems for Electric and Hybrid Vehicle Battery Packs*," presented at the Fourth Vehicle Thermal Management Systems Conference and Exhibition, London, UK, May 24-27, 1999.

28. Incropera, F.P. & De Witt, D.P., "Fundamentals of Heat and Mass Transfer," John Wiley and Sons, ISBN 0-471-30460-3, 1996.

29. Zhukauskas, A., & Ulinskas, R., "Heat Transfer in Tube Banks in Crossflow,": Hemisphere Pub. Corp., New York, ISBN 0-89116-685-8, 1988

CONTACT INFORMATION

Tugce Yuksel
Research Assistant
Department of Mechanical Engineering
Carnegie Mellon University
Pittsburgh, PA 15213
tyuksel@andrew.cmu.edu

Jeremy Michalek
Associate Professor
Department of Mechanical Engineering
Department of Engineering and Public Policy
Carnegie Mellon University
Pittsburgh, PA 15213
jmichalek@cmu.edu

ACKNOWLEDGMENTS

The authors wish to thank Professor Shawn Litster and the members of the Vehicle Electrification Group and the Design Decisions Laboratory at Carnegie Mellon University; Dr. Kandler Smith and Dr. Shriram Santhanagopalan at the National Renewable Energy Laboratory; Dr. Ted Miller at Ford Motor Company; Mr. Bill Reinert, Mr. Jeffrey Makarewicz and Dr. Monique Richard at Toyota Motor Corporation; Mr. Oliver Gross at Chrysler Group LLC; and Dr. Philip Stephenson and Dr. Yang Chen at A123 Systems, Inc. for their valuable guidance, suggestions, and feedback. This work was supported in part by a Fulbright grant from the U.S. Department of State Bureau of Educational and Cultural Affairs, a grant from the National Science Foundation CAREER program #0747911, and a grant from Toyota Motor Corporation. Any opinions, findings, and recommendations expressed are those of the authors and do not necessarily reflect the views of the sponsors.

ISSN 0148-7191

SAE Customer Service:
Tel: 877-606-7323 (inside USA and Canada)
Tel: 724-776-4970 (outside USA)
Fax: 724-776-0790
Email: CustomerService@sae.org
SAE Web Address: http://www.sae.org
Printed in USA